The role of hydrogen flow rates in the direct reduction of iron ore pellets: Investigating external mass transfer limitations

M.L. Ali[1*], S. Fong[1], Q. Fradet[1] and U. Riedel[1]

*E-Mail: mohammed.ali@dlr.de

[1]German Aerospace Center (DLR), Institute of Low-Carbon Industrial Processes,
Äußere Oybiner Straße 14/16, 02763 Zittau, Germany

Abstract

The successful transition to hydrogen-based direct reduction in ironmaking demands an in-depth comprehension of the complex reaction mechanisms and mass transfer dynamics at play. While high hydrogen flow rates in the reduction of single iron ore pellets are commonly used for mechanism development to neglect external mass transfer effects for simplification, this study critically examines the reduction behavior under low hydrogen flow conditions, where external mass transfer becomes significant, mirroring practical conditions more closely. Thermogravimetric analysis (TGA) experiments were conducted at 1073 K, 1173 K, and 1273 K, with H_2 flow-rates of 100 and 300 mL/min, revealing increased external mass transfer resistance at lower flow rates and higher temperatures. To numerically investigate this heterogeneous reacting system, a coupled 1D solid porous and 3D CFD modeling framework is employed, iteratively exchanging data of kinetic rates and gas concentrations at the pellet surface and validating the predictions against experimental data. This work advances reliable kinetic mechanisms for hydrogen-based reduction, addressing model scalability challenges.

Introduction

The steel industry is a substantial contributor to global CO_2 emissions, necessitating urgent decarbonization strategies aligned with climate goals. Hydrogen-based direct reduction (H_2-DR) offers a viable low-carbon alternative to conventional processes [1]. Single-pellet studies often neglect external mass transfer effects by using high flow rates [2]. While this simplifies modeling activities, relevance for industrial applications is limited, as real moving-bed systems exhibit localized flow effects, and steam, the inherent reaction product of the reduction, is abundantly present [3,4]. These conditions create mass transfer and chemical resistance, impacting the overall reduction rates and process efficiency. Models neglecting these effects will fail to predict furnace behavior at industrial-scales.

This study aims to develop a reliable kinetic mechanism for the reduction of single iron ore pellets under low H_2 flow-rates, explicitly addressing external mass transfer limitations. A 1D solid porous model [5] predicts reaction rates by solving mass conservation equations within the pellet, accounting for internal diffusion, porosity, and heterogeneous chemistry. A 3D CFD model [3] resolves gas flow and species concentrations throughout the pellet and reactor domain, resolving external mass transfer resistance. Through iterative data exchange, the coupled models ensure consistent and accurate kinetic predictions. The predictions of the coupled models will be validated against TGA-experiment results at various temperature and flow rates.

Experimental and Modeling Approach

Reduction experiments were conducted using a Linseis PT1600 TGA system on single DR-grade iron ore pellets (11.5 mm diameter, 27% porosity) in an H_2 atmosphere at 1073 K, 1173 K, and 1273 K, with flow rates of 100 and 300 mL/min. The setup featured a vertical furnace for uniform heating, an inert N_2 purge system to prevent oxidation, precise gas flow controllers, and a programmable temperature controller for accurate isothermal holds. The pellets were suspended on a quartz holder to ensure consistent gas exposure.

The H_2-DR modeling employed a 1D solid porous model and a 3D CFD model. The solid porous model was developed to circumvent the limitations of the traditional shrinking core model and its incompatibility with discretized CFD frameworks. The 1D model, assuming a spherical symmetry, solves the gas concentrations, the solid mass fractions, and the porosity across the pellet radius as a function of time, capturing intrinsic reaction kinetics. However, since the 1D model considers only the pellet as the computational domain, it cannot resolve the external mass transfer. To address this, the 3D-CFD model was developed using a self-implemented solver in OpenFOAM, covering the entire reactor domain, including both the pellet and the surrounding gas flow. The models iteratively exchange information, with the 3D-CFD model providing external boundary conditions and the 1D model supplying reaction rates. Both models share governing equations for mass conservation, momentum conservation, species transport, and solid mass fraction evolution as shown in **Table 1**.

Table 1. Governing Equations in 1D and CFD models

1D	Gas concentration	$\frac{\partial C_i}{\partial t} = \frac{1}{\varepsilon}\nabla \cdot \left(D^{\mathrm{eff}}\nabla C_i\right) + \frac{1}{\varepsilon}\dot{s}_i - \frac{C_i}{\varepsilon}\frac{\partial \varepsilon}{\partial t}$	(1)
1D/CFD	Solid mass fraction	$\frac{\partial X_j}{\partial t} = \frac{1}{1-\varepsilon}\frac{M_j}{\rho_j}\dot{\mathrm{s}}_j + \frac{X_j}{1-\varepsilon}\frac{\partial \varepsilon}{\partial t}$	(2)
1D/CFD	Porosity	$\frac{\partial \varepsilon}{\partial t} = -\sum_j \frac{M_j}{\rho_j}\dot{\mathrm{s}}_j$	(3)
CFD	Gas Continuity	$\frac{\partial \alpha_{\mathrm{g}}\rho_{\mathrm{g}}}{\partial t} + \nabla \cdot \left(\rho_{\mathrm{g}}\mathbf{v}_{\mathrm{g}}\right) = S_{\mathrm{g}}$	(4)
CFD	Gas Momentum	$\frac{\partial \alpha_{\mathrm{g}}\rho_{\mathrm{g}}\mathbf{v}_{\mathrm{g}}}{\partial t} + \nabla \cdot \left(\rho_{\mathrm{g}}\mathbf{v}_{\mathrm{g}}\mathbf{v}_{\mathrm{g}}\right) = \nabla \cdot \bar{\bar{\tau}} - \nabla p + \rho_{\mathrm{g}}\mathbf{g} + \mathbf{M}_{\mathrm{sg}}$	(5)
CFD	Gas species transport	$\frac{\partial \alpha_{\mathrm{g}}\rho_{\mathrm{g}}Y_{\mathrm{g},i}}{\partial t} + \nabla \cdot \left(\rho_{\mathrm{g}}Y_{\mathrm{g},i}\mathbf{v}_{\mathrm{g}}\right) = -\nabla \cdot \mathbf{j}_{\mathrm{g},i}^{\mathrm{eff}} + M_i\dot{\omega}_i + M_i s_i$	(6)

The gaseous reduction of iron ore occurs in the sequence: Fe_2O_3 (hematite) → Fe_3O_4 (magnetite) → FeO (wüstite) → Fe (metallic iron). The reactions in a pure hydrogen atmosphere above 840 K proceed as follows:

$$3\,Fe_2O_{3(s)} + H_{2(g)} \rightarrow 2\,Fe_3O_{4(s)} + H_2O_{(g)}, \tag{7}$$

$$Fe_3O_{4(s)} + H_{2(g)} \rightarrow 3\,FeO_{(s)} + H_2O_{(g)}, \tag{8}$$

$$FeO_{(s)} + H_{2(g)} \rightleftharpoons Fe_{(s)} + H_2O_{(g)}. \tag{9}$$

The backward reaction of equations (7) and (8) have been omitted, but not for equation (9), as the reverse rate is supposedly non-negligible.

Results and Discussions

The main evaluation criterion for model validation is the global conversion degree *F*, given by:

$$F = \frac{m_0 - m(t)}{m_0 - m_\infty}. \tag{10}$$

Here, m_0 represents the initial mass of the pellet, $m(t)$ is the mass at a given time *t*, and m_∞ corresponds to the theoretical mass after complete reduction. The value of *F* ranges from 0, indicating no conversion (Fe_2O_3 and gangue), to 1, indicting complete conversion (Fe and gangue).

Figure 1 demonstrates the effect of H_2 flow rates on the reduction kinetics of single iron ore pellets at various temperatures. **Figure 1** (a-c) show the conversion degree of the TGA experiments at 1073 K, 1173 K, and 1273 K, respectively. Higher flow rates (300 mL/min) consistently lead to a faster reduction. **Figure 1** (e) represents the TGA device arrangement and the gas flow dynamics around the pellet obtained by the CFD simulation. A close-up view at 300 seconds of the hydrogen mole fraction contour is given in **Figure 1** (d) for the two tested gas flow rate, 100 and 300 mL/min. The H_2 concentration in the gas phase is lower for the 100 mL/min flow rate due to greater external transport limitations. In addition, the concentration of hydrogen inside the pellet is also lower, which decrease the forward reduction rates and increase the rate of the reverse reaction between iron and wüstite. An inflection point is clearly visible in the experiments using 100 mL/min at around 30% conversion, which corresponds to the reduction from up to wüstite. After this point, the global conversion is controlled mostly by the equilibrium reaction (9) and by the flushing rate of water out of the pellet and subsequently out of the reactor. Only at the final reduction stage, where oxides near the pellet surface are depleted, does the system transition to a diffusion-controlled regime.

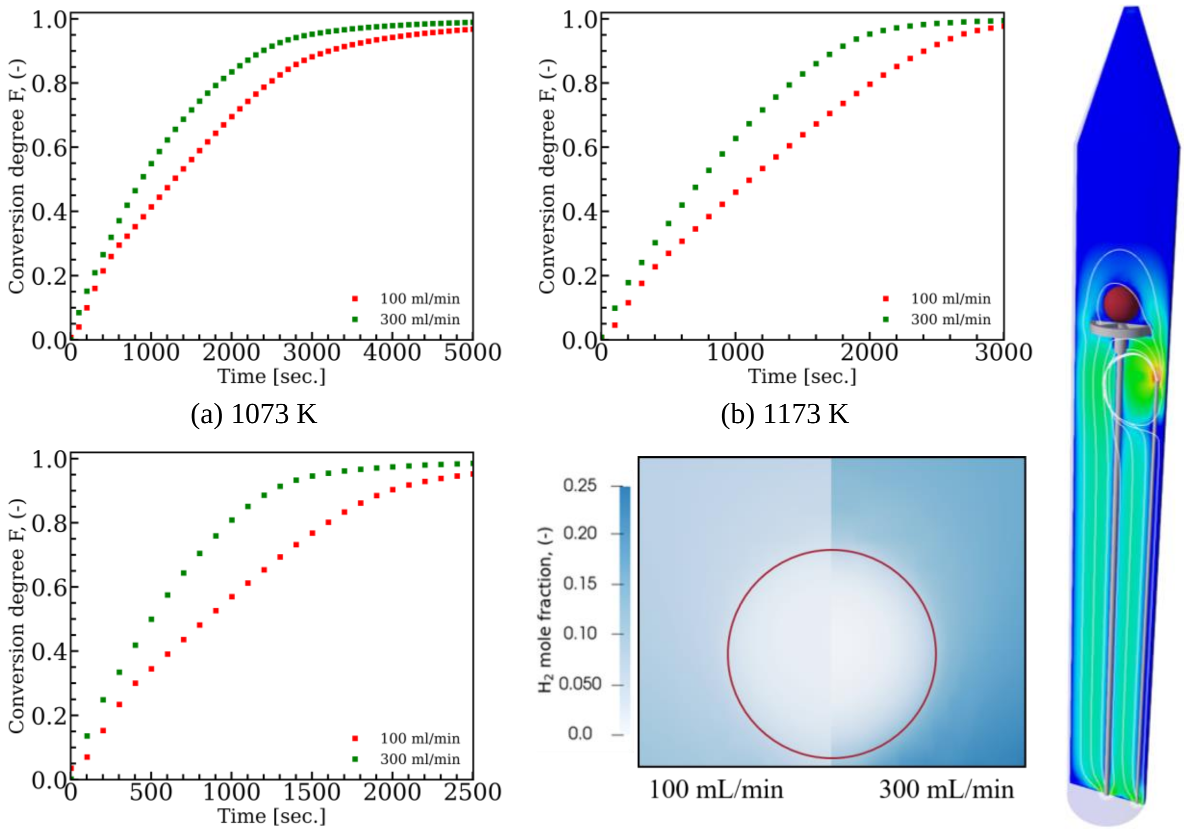

(a) 1073 K

(b) 1173 K

(c) 1273 K

(d) 1173 K

(e)

Figure 1. (a-c) Overall conversion degree over time for two flow rates and three different temperatures. (d) Contour plot of H_2 mole fraction inside and around the pellet at 1173 K at flow rates of 100 mL/min (left) and 300 mL/min (right). (e) CFD simulation showing velocity gradient and streamlines around a single iron ore pellet in the TGA furnace.

As previously described, the reduction process involves a complex interplay between flow field, internal diffusion, and reaction kinetics. The experimental and numerical methodology conducted here will allow to decouple all these effects. The next step is to forward the boundary condition information, as exemplary given in **Figure 1** (d), to the 1D model. The use of various temperatures and H_2/H_2O ratios at the boundary, while keeping other parameters (such as the pellet properties) constant, will allow to accurately determine kinetic parameters of both forward and backward reduction reactions. Such a robust kinetic mechanism is a pre-requisite to CFD simulations of multiple pellet cases.

Acknowledgements

We acknowledge funding by the European Union and by tax revenues on the basis of the budget adopted by the Saxon State Parliament. European Regional Development Fund (EFRE) project “BioFe - Biomassenutzung in der Eisenerzeugung unter wirtschaftlichen und CO_2-mindernden Randbedingungen”.

References

[1] World Economic Forum. *Which technologies will enable a cleaner steel industry?* Available from: https://www.weforum.org/stories/2024/04/technologies-cleaner-steel-industry/, 2024.

[2] Kazemi M., Pour M., Sichen D.: *Experimental and Modeling Study on Reduction of Hematite Pellets by Hydrogen Gas*, Metall. Mater. Trans. B, 48, 2, 2017.

[3] Ali M. L., Fradet Q., Riedel U.: *Particle-resolved computational modeling of hydrogen-based direct reduction of iron ore pellets in a fixed bed. Part I: Methodology and validation*, International Journal of Hydrogen Energy, 87, 2024.

[4] Ali M. L., Mehlhose S., Fradet Q., Riedel U.: *Particle-resolved computational modeling of hydrogen-based direct reduction of iron ore pellets in a fixed bed. Part II: Influence of the pellet sizes and shapes*, International Journal of Hydrogen Energy, 86, 2024.

[5] Fradet Q., Ali M. L., Riedel U.: *Development of a Porous Solid Model for the Direct Reduction of Iron Ore Pellets*, Steel Research International, 93, 12, 2022.